

# 10.5 THE GLOBAL SURFACE AND ATMOSPHERE RADIATION BUDGET: AN ASSESSMENT OF ACCURACY WITH 5 YEARS OF CALCULATIONS AND OBSERVATIONS

Thomas P. Charlock\*, Fred G. Rose, David A. Rutan, Zhonghai Jin, and Seiji Kato

## 1. Introduction

We compute the surface and atmosphere radiation budget (SARB) and validate with simultaneous, collocated broadband observations at top of atmosphere (TOA) and surface. The differences of TOA and surface fluxes determine the net radiative cooling of the atmosphere. If known accurately over the globe at all times, this net radiation would balance the sum of the global mean latent and sensible heating - other benchmarks sought by the GCM and climate diagnostics community. Our radiative transfer calculations are a bit more sophisticated than those in GCMs. By comparing computations and observations at TOA and surface, we find specific examples of the strengths and weaknesses of the radiative transfer code, the inputs for the code, and the satellite and ground-based broadband fluxes.

While mainly intended to provide observations of TOA fluxes, the Clouds and the Earth's Radiant Energy System (CERES, Wielicki, et al, 1996) includes a program to compute the fluxes at TOA, within the atmosphere and at the surface, and also to validate with independent ground based measurements (Charlock and Alberta, 1996). The multi-year computed SARB described here is archived as Terra CRS Edition 2B (ungridded snapshots at satellite overpass) and Terra FSW Edition 2C (gridded and placed in the hour-box closest to overpass); it does not yet span the entire diurnal cycle. Related papers in this volume by Rose et al (2006) describe a preliminary version of a CERES SARB that uses geostationary data to cover the diurnal cycle; a finished, gridded surface albedo product that is available on the web (Rutan et al, 2006a); an ocean surface surface albedo tool that is suitable for GCMs, as well as remote sensing (Jin et al, 2006); and a more advanced radiative transfer code for the next generation of CERES products (Rose et al. 2006b).

## 2. Calculation of Fluxes

We use a fast, plane parallel correlated-k radiative transfer code based on (Fu and Liou, 1993, Fu et al., 1997, 1998) which has been highly modified

and now dubbed the "Langley Fu-Liou code". A 2 stream calculation is used for SW with 15 bands. LW employs a 2/4 stream version, wherein the source function is evaluated with the quick 2-stream approach, while radiances are effectively computed at 4 streams. Constituents for the thermal infrared include H<sub>2</sub>O, CO<sub>2</sub>, O<sub>3</sub>, CH<sub>4</sub> and N<sub>2</sub>O. A special treatment of the CERES 8.0-12.0  $\mu$ m window includes CFCs (Kratz and Rose, 1999) and uses the Clough CKD 2.4 version of the H<sub>2</sub>O continuum. The HITRAN2000 data base was used for the determination of correlated k's in the SW (Kato et al., 1999). We make a first order accounting for inhomogeneous cloud optical thickness by using the gamma weighted two stream approximation (GWTS) of Kato et al. (2005) in the SW. An external mixture of aerosols, clouds, and gases is assumed. All-sky aerosol forcing is determined by running with clouds (if present), gases, and aerosols, and subtracting the flux from a run with no aerosols. A theoretical clear-sky aerosol forcing is computed for all footprints as the difference of the cloud-free flux with aerosols minus the cloud-free flux with no aerosols. Aerosol forcing includes the effects scattering (SW and LW), absorption (SW and LW) and emission (LW) by aerosols.

The major inputs to the flux calculation are retrievals of cloud area, height, optical depth, particle size and phase from small (<1 km) MODIS pixels (Minnis et al., 2002); gridded temperature, humidity, surface wind (GEOS4, Bloom et al, 2004); and ozone from NCEP (Yang et al., 2000). SARB fluxes are calculated for each large (~20 km) footprint of the broadband CERES instrument, which provides observed TOA fluxes.

Land surface albedo is explicitly retrieved for clear footprints using a quick look-up table (LUT) to the Langley Fu-Liou code that relates observed CERES TOA albedo, surface albedo, solar zenith angle (SZA), precipitable water, and aerosol optical thickness (AOT). In computing the LUT, the spectral *shape* of land surface albedo is assumed as per the International Geophysical Biospherical Project (IGBP) land type (see <http://www-surf.larc.nasa.gov/surf/>); the spectral shapes of sea ice and snow are assumed from theoretical calculations of Jin and Stamnes (1994). When cloudy, the land surface albedo is taken from a gridded record of clear-sky retrievals during the same month; and adjusted to account for an effective diffuse solar zenith angle (SZDA) beneath clouds. Because of uncertainties in the cloud optical depth retrieval over the cryosphere, the

---

\*Corresponding author address: Thomas P. Charlock, Mail Stop 420, NASA Langley Research Center, Hampton, Virginia 23681; e-mail: Thomas.P.Charlock@nasa.gov

surface albedo of cloudy footprints (for optical depth below 20) with snow or ice are retrieved with CERES data and a LUT. The spectral albedo of the ice-free ocean, however, is obtained using a LUT based on discrete ordinate calculations with a sophisticated coupled ocean atmosphere radiative transfer code (Jin et al, 2004). Inputs for ocean spectral albedo include SZA, wind speed, chlorophyll concentration (which has a minor effect on broadband flux), and SW optical depth of clouds and aerosols. There is an empirical correction for surface foam based on wind speed.

AOT is taken from MODIS (MOD04 described by Kaufman et al., 1997) when available. Over the ocean, MOD04 is used for 7 wavelengths; the AOT is interpolated to the remainder of the spectrum using the selected aerosol type, as specified below. Over the land, MOD04 provides AOT at 3 wavelengths, and the MOD04 Angstrom exponent is used to guide the extension over the spectrum. If the MOD04 instantaneous AOT is not available (i.e., footprint is overcast), we temporally interpolate from a file of the MODIS Daily Gridded Aerosol. When cloudiness in the footprint exceeds 50%, or when there is no MODIS AOT, we use AOT from the NCAR MATCH (Collins et al., 2001). When AOT is taken from MATCH, we assume it for one wavelength only (0.63 $\mu$ m). MATCH AOT is apportioned to 7 types (small dust, large dust, soot, soluble organic, insoluble organic, sulfate, and sea salt) on a daily basis over the globe for all sky conditions. Aerosol type is always taken from MATCH; this guides the selection of the asymmetry factor ( $g$ ) and the single scattering albedo (SSA). Asymmetry factors and SSA are assumed from the Tegen and Lacis (1996), Lacis (personal communication, 2004), and OPACS-GADS (Hess et al., 1998) models.

For each CERES cross track footprint on Terra, the Langley Fu-Liou radiative transfer code is run for profiles of SW and LW fluxes; and aerosol and cloud forcings at surface and TOA. Results at the time of Terra overpass are in the public archive over the globe for March 2000 to June 2005. Except for the determination of surface albedo over land and the cryosphere, CERES broadband observations are not used as inputs for the "untuned" version of these calculations. "Tuned" calculations are made by adjusting inputs to produce a closer match of broadband computations and observations at TOA. No broadband radiometric observations at the surface are used for radiative transfer inputs, adjustments, or tuning; the flux comparison at the surface in the next section is a "cold" test. We focus on untuned results here.

### 3. Validation at Ground Sites

This summary table for 2001 (NOT corrected for official CERES Rev1 instrument adjustments to SW at TOA) at a representative group of BSRN, SURFRAD, and ARM ground sites is from the URL

[www-cave.larc.nasa.gov/cave](http://www-cave.larc.nasa.gov/cave). "Obs" denotes mean observed value ( $Wm^{-2}$ ). Bias as untuned calculation minus observation ( $Wm^{-2}$ ) at  $\sim 1030$  L and  $\sim 2230$  L Terra overpasses. SFC denotes surface.

Parameter\_\_\_\_Obs\_\_\_\_Bias\_\_\_\_N

All-sky  
 LW down SFC 286.1 -6.1 22420  
 LW up\_\_ SFC 353.5 -3.6 10938  
 SW down SFC 444.3 13.1 11204  
 SW up\_\_ SFC 112.8 -18.4 5152  
 LW up\_\_ TOA 218.8 1.4 22885  
 SW up\_\_ TOA 261.0 10.7 10873

Clear-sky  
 LW down SFC 291.5 -8.7 3500  
 LW up\_\_ SFC 400.0 -0.7 2263  
 SW down SFC 726.1 -0.4 1801  
 SW up\_\_ SFC 154.1 -22.7 1048  
 LW up\_\_ TOA 274.8 -0.3 3597  
 SW up\_\_ TOA 196.5 -0.2 1844

The computed LW down SFC has an all-sky (clear-sky) bias of  $-6.1 Wm^{-2}$  ( $-8.7 Wm^{-2}$ ); the main cause is the GEOS-4 input for surface air temperature (it's too cold). The skin temperature retrieved by CERES from MODIS (Minnis et al, 2002) is great: the clear-sky bias for LW up SFC is only  $-0.7 Wm^{-2}$ . The clear-sky bias for insolation SW down SFC is only  $-0.4 Wm^{-2}$ ; a small bias is obtained at many individual sites, suggesting good inputs for aerosols in the time mean (this holds up for many sites in the annual mean, but it does not for others). The large biases for SW up SFC mean that the retrieved surface albedo needs some explanation. The bias for SW up TOA is  $10.7 Wm^{-2}$ , which is almost 4%. The application of SARB "tuning" (not shown in Table 1) reduces the bias in SW up TOA but increases the bias in SW down SFC for cloudy sky. By applying a new "Rev1" adjustment to the CERES SW record (Matthews and Priestley, 2006), as officially recommended by the Science Team, the discrepancy of almost 4% in 2001 would still remain above 3%.

### 4. Computed and Observed TOA Fluxes over the Globe

In the global mean (rather than just at the ground sites above), computed SW reflection to TOA ( $251.5 Wm^{-2}$ ) exceeds CERES observations ( $241.5 Wm^{-2}$ ) by over 4% during March 2003 (Figure 1).

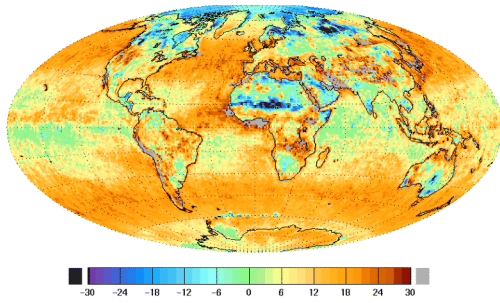


Figure 1. Bias in reflected SW at TOA as Untuned Calculation minus Observation at on a scale -30 to 30 Wm<sup>-2</sup>. March 2003 daytime overpass as CERES Terra FM1 FSW Ed 2C.

The corresponding bias for outgoing longwave (OLR) is negligible, when averaged over the globe for both day and nite (Figure 2). But regional biases in the computed OLR are apparent.

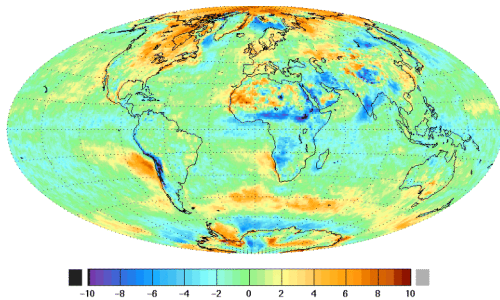


Figure 2. Bias in OLR as Untuned Calculation minus Observation at on a scale -10 to 10 Wm<sup>-2</sup>. March 2003 day and nites overpasses as CERES Terra FM1 FSW Ed 2C.

The relative SW bias is diagnosed in Figure 3, which isolates overcast clouds only for a single day (1 July 2000) over the ice-free oceans. Here the inputs for the computed SW are not influenced at all by the value of the SW observed by the broadband CERES instrument. Relative biases for overcast ice and liquid clouds have been separately plotted; each bin (a point for liquid or a circle for ice) represents the bias for hundreds of footprints. The bias is small only for clouds with optical thickness over about 50. For optically thin clouds, the relative biases easily exceed 0.05 (5%).

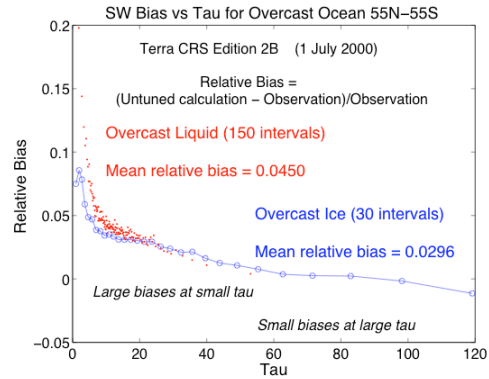


Figure 3. Relative bias in reflected SW at TOA as ratio of (Untuned Calculation minus Observation) to (Observation) for overcast clouds over the oceans. 1 July 2000 daytime overpass as CERES Terra FM1 CRS Ed2B.

The relative SW bias of the untuned calculations is explored as a deseasonalized time series in Figure 4. All data in Figure 4 are based on raw monthly footprint means of ungridded CRS data (Figures 1 and 2 use gridded FSW data). The dashed lines use the official untuned product. Note the dashed blue lines for the clear ocean. Here the computed flux depends on the parameterization of Rayleigh scattering and the input values for ocean surface albedo, both of which validate well with special measurements at individual surface sites. The relative bias for clear SW in July 2000 is about 0.01 (1%) in Figure 4. Hence the large bias for low optical depth clouds (Figure 3) is likely not due to the clear sky component of the parameterization.

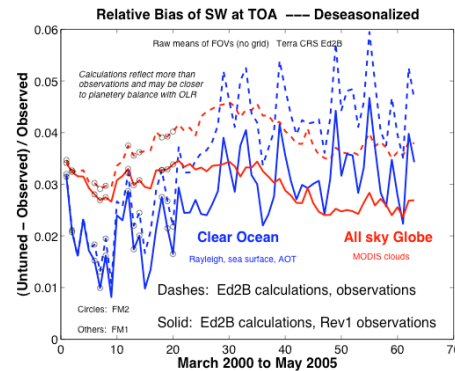


Figure 4. Relative bias in reflected SW at TOA as ratio of (Untuned Calculation minus Observation) to (Observations). Biases of official, untuned calculations (CRS Ed2B) are dashed. Biases corrected with Rev 1 adjustments to observations in solid. All-sky for combined land and sea in red. Clear ocean only in blue.

The solid lines in Figure 4 (red for all-sky over land and sea and blue for clear ocean only) assess the relative bias with the latest "Rev 1" correction to the CERES measurements (Matthews

and Priestley, 2006). Rev 1 was not available when the calculations were done. Both the all-sky (red) and clear ocean (blue) untuned calculations show a mean relative bias of ~3% for the 5 year interval, but the clear ocean bias is more highly variable. The Rev 1 adjustments to the CERES measurements (solid) have reduced the bias. The large trend for clear ocean is disconcerting; the small variations in the inputs for the calculation over the 5-year period (i.e., aerosol optical thickness from MODIS) cannot explain it.

Trends in the deseasonalized bias for OLR, here as an absolute bias in  $Wm^{-2}$ , are much smaller (Figure 5). The day (1  $Wm^{-2}$ ) and nite (-1  $Wm^{-2}$ ) all-sky biases compensate. There is a long-term drift in the all-sky OLR bias during the day, but not in the all-sky OLR bias during the nite, and not in the window portion of the OLR (which CERES measures with an independent instrument). The observed OLR is here based on a difference of an "all wave" (SW plus LW) channel and a SW channel. A Rev 1 adjustment is available for the SW observation, but not for the OLR. Further instrument adjustments may be needed. The calculation does not account for changes in  $CH_4$  and  $N_2O$ , but such changes are too small to explain solid blue line in Figure 5.

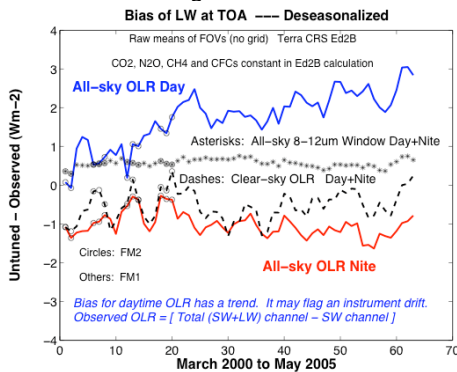


Figure 5. Bias in emitted LW at TOA (Untuned Calculation minus Observation) to (Observations).

While absolute biases for reflected SW and OLR, and the trends in some biases, are not fully explained, there is much more confidence in the geographical patterns of changes in radiation. Figure 6a shows the difference in the reflected SW at TOA from the untuned calculations of March 2002 and March 2003; they differ by only 0.6  $Wm^{-2}$  for the global mean but show rich patterns of regional variation. The match with the observed version (Figure 6b), where the two months differ by 0.8  $Wm^{-2}$  for the global mean, is striking.

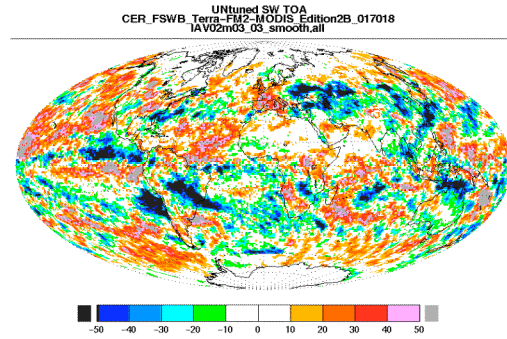


Figure 6a. Difference in computed reflected SW at TOA (March 2002 - March 2003) on a scale -50 to 50  $Wm^{-2}$ .

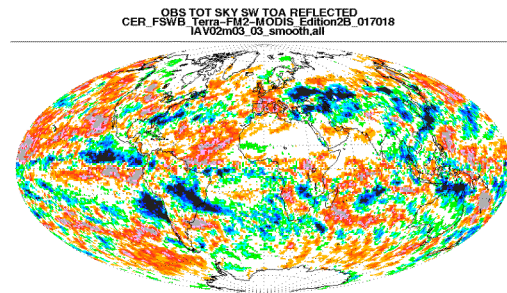


Figure 6b. Observed difference in reflected SW at TOA (March 2002 - March 2003) on a scale -50 to 50  $Wm^{-2}$ .

## 5. Discussion

A comparison of the computed and observed fluxes at surface and TOA is a resource for assessing the fidelity of our values for the components of the current earth radiation budget, changes in that budget, and factors associated with the changes. The results here cover the satellite overpass snapshots only; they are not complete; many assumptions in the calculations were simple. The most notable discrepancy at this stage is perhaps that between calculations and observations for SW in cloudy sky. An error of this scale - about 3% at TOA - could be due to several factors, including the simplified scheme for broadband radiative transfer, the MODIS input data used to retrieve cloud optical properties, the assumptions in the cloud optical property retrieval, the inversion from measured radiance to observed flux, or procedures that yield CERES radiances. It is significant, because if the earth were to suddenly reflect 3% more SW than it does at present, the planet would be out of radiative balance by ~7  $Wm^{-2}$ ; and for the global annual mean of recent decades, we have surely have no such imbalance. Resolving the differing trends for components of computed and observed SW (Figure 4) and LW (Figure 5) may even more important for the

interpretation of climate change. The URL <http://www-cave.larc.nasa.gov/cave/> provides access to much of the data used in this analysis, as well as to "point and click" versions of the radiative transfer codes.

## 6. References

- Bloom, S., A. da Silva, D. Dee, M. Bosilovich, J.-D. Chern, S. Pawson, S. Schubert, M. Sienkiewicz, I. Stajner, W.-W. Tan, M.-L. Wu, 2005: Documentation and Validation of the Goddard Earth Observing System (GEOS) Data Assimilation System - Version 4 . Technical Report Series on Global Modeling and Data Assimilation 104606 , 26. Document (18124 kb) <http://gmao.gsfc.nasa.gov/systems/geos4/>
- Charlock, T. P., and T. L. Alberta, 1996: The CERES/ARM/GEWEX Experiment (CAGEX) for the retrieval of radiative fluxes with satellite data. *Bull. Amer. Meteor. Soc.*, **77**, 2673-2683.
- Collins, W. D., P. J. Rasch, B. E. Eaton, B. V. Khattatov, J.-F. Lamarque, and C. S. Zender, 2001: Simulating aerosols using a chemical transport model with assimilation of satellite aerosol retrievals: Methodology for INDOEX. *J. Geophys. Res.*, **106**, 7313-7336.
- Fu, Q., and K.-N. Liou, 1993: Parameterization of the radiative properties of cirrus clouds. *J. Atmos. Sci.*, **50**, 2008-2025.
- Fu, Q., K. Liou, M. Cribb, T. Charlock, and A. Grossman, 1997: On multiple scattering in thermal infrared radiative transfer. *J. Atmos. Sci.*, **54**, 2799-2812.
- Fu, Q., G. Lesins, J. Higgins, T. P. Charlock, P. Chylek, and J. Michalsky, 1998: Broadband water vapor absorption of solar radiation tested using ARM data. *Geophys. Res. Lett.*, **25**, 1169-1172.
- Hess, M., P. Koepke, and I. Schult, 1998: Optical Properties of Aerosols and Clouds: The software package OPAC. *Bull. Amer. Meteor. Soc.*, **79**, 831-844.
- Jin, Z., and K. Stamnes, 1994: Radiative transfer in nonuniformly refracting layered media: Atmosphere-ocean system. *Appl. Opt.*, **33**, 431-442.
- Jin, Z., T. P. Charlock, W. L. Smith, Jr., and K. Rutledge, 2004: A look-up table for ocean surface albedo. *Geophys. Res. Lett.*, **31**, L22301.
- Jin, Z., T. P. Charlock, and K. Rutledge, 2006: A parameterization of spectral ocean surface albedo (OSA) for climate models. Proceedings of 12<sup>th</sup> Conference on Atmospheric Radiation (AMS), 10-14 July 2006, Madison, Wisconsin.
- Kato, S., T. P. Ackerman, E. G. Dutton, N. Laulainen, and N. Larson, 1999: A comparison of modeled and measured surface shortwave irradiance for a molecular atmosphere, *J. Quant. Spectrosc. Radiat. Transfer.*, **61**, 493-502.
- Kato, S., F. G. Rose, and T. P. Charlock, 2005: Computation of domain-averaged irradiance using satellite-derived cloud properties. *J. Atmos. Ocean. Tech.*, **22b**, 146-164.
- Kaufman, Y. J., D. Tanre, H. R. Gordon, T. Nakajima, J. Lenoble, R. Frouin, H. Grassl, B. M. Herman, M. D. King, and P. M. Teillet, 1997: Passive remote sensing of tropospheric aerosol and atmospheric correction for the aerosol effect. *J. Geophys. Res.*, **102**, 16,815-16,830.
- Kratz, D. P., and F. G. Rose, 1999: Accounting for molecular absorption within the spectral range of the CERES window channel. *J. Quant. Spectrosc. Radiat. Transfer*, **48**, 83-95.
- Matthews, G., and K. Priestley, 2006: CERES Edition 2 Rev 1 Calibration Adjustments to Compensate for Shortwave Spectral Darkening of Optics. Proceedings of 12<sup>th</sup> Conference on Atmospheric Radiation (AMS), 10-14 July 2006, Madison, Wisconsin.
- Minnis, P., D. F. Young, B. A. Wielicki, D. P. Kratz, P. W. Heck, S. Sun-Mack, Q. Z. Trepte, Y. Chen, S. L. Gibson, and R. R. Brown: 2002: Seasonal and Diurnal Variations of Cloud Properties Derived from VIRS and MODIS Data. Extended abstract for 11<sup>th</sup> Conference on Atmospheric Radiation (AMS), 3-7 June 2002 in Ogden, Utah.
- Rose, F., T. Charlock, Q. Fu, S. Kato, D. Rutan, and Z. Jin, 2006: CERES Proto-Edition 3 Radiative Transfer: Tests and Radiative Closure over Surface Validation Sites. Proceedings of 12<sup>th</sup> Conference on Atmospheric Radiation (AMS), 10-14 July 2006, Madison, Wisconsin.
- Rose, F., T. Charlock, B. Wielicki, D. Doelling, and S. Zentz, 2006: CERES Synoptic Gridded Diurnally Averaged Radiative Transfer. Proceedings of 12<sup>th</sup> Conference on Atmospheric Radiation (AMS), 10-14 July 2006, Madison, Wisconsin.
- Rutan, D., T. Charlock, F. Rose, S. Kato, S. Zentz, and L. Coleman, 2006: Global Surface Albedo from CERES/TERRA Surface and Atmospheric Radiation Budget (SARB) Data Product. Proceedings of 12<sup>th</sup> Conference on Atmospheric

Radiation (AMS), 10-14 July 2006, Madison, Wisconsin.

Tegen, I., and A. A. Lacis, 1996: Modeling of particle size distribution and its influence on the radiative properties of mineral dust aerosol. *J. Geophys. Res.*, **101**, 19,237-19,244.

Wielicki, B. A., B. R. Barkstrom, E. F. Harrison, R. B. Lee, G. L. Smith, and J. E. Cooper, 1996: Clouds and the Earth's Radiant Energy System (CERES): An Earth Observing System Experiment. *Bull. Amer. Meteor. Soc.*, **77**, 853-868.

Yang, S.-K., S. Zhou, and A. J. Miller, 2000: SMOBA: A 3-D daily ozone analysis using SBUV/2 and TOVS measurements. [www.cpc.](http://www.cpc.ncep.gov/products/stratosphere/SMOBA/smoba_doc.html)

[ncep.gov/products/stratosphere/SMOBA/smoba\\_doc.html](http://www.cpc.ncep.gov/products/stratosphere/SMOBA/smoba_doc.html)

## 6. Acknowledgements

ARM data is made available through the U.S. Department of Energy as part of the Atmospheric Radiation Measurement Program.

CMDL data is made available through the NOAA/CMDL Solar and Thermal Radiation. (STAR) group.

SURFRAD data is made available through NOAA's Air Resources Laboratory/Surface Radiation Research Branch